J Appl Physiol 97: 1567–1574, 2004.
First published June 18, 2004; 10.1152/japplphysiol.00396.2004.

HIGHLIGHTED TOPIC | *Lung Growth and Repair*

Regional lung growth following pneumonectomy assessed by computed tomography

Priya Ravikumar,[1] Cuneyt Yilmaz,[1] D. Merrill Dane,[1] Robert L. Johnson, Jr.,[1] Aaron S. Estrera,[2] and Connie C. W. Hsia[1]
(With the Technical Assistance of Richard T. Hogg and Deborah C. Hogg)
Departments of [1]Internal Medicine and [2]Cardiovascular and Thoracic Surgery, University of Texas Southwestern Medical Center, Dallas, Texas 75390-9034

Submitted 12 April 2004; accepted in final form 6 June 2004

Ravikumar, Priya, Cuneyt Yilmaz, D. Merrill Dane, Robert L. Johnson, Jr., Aaron S. Estrera, and Connie C. W. Hsia. Regional lung growth following pneumonectomy assessed by computed tomography. *J Appl Physiol* 97: 1567–1574, 2004. First published June 18, 2004; 10.1152/japplphysiol.00396.2004.—After pneumonectomy (PNX), mechanical strain on the remaining lung is greatly increased. To assess whether remaining lobes expand uniformly after left or right PNX (removing 42 and 58% of lung mass, respectively), we performed high-resolution computed tomography (CT) scans at 45 ml/kg above end-expiratory lung volume on adult male foxhounds after left or right PNX, which were compared with adult Sham controls. Air and tissue volumes were separately measured in each lobe. After left PNX, air and tissue volumes in the right upper and cardiac lobes increased ~2.2-fold above and below the heart, whereas volumes in right middle and lower lobes did not change significantly. After right PNX, air and tissue volumes in the left upper and middle lobes increased 2.3- to 2.7-fold across the midline anterior to the heart, whereas the left lower lobe expanded ~1.9-fold posterior to the heart. Regional changes in volume density of tissue post-PNX estimated by CT scan parallel postmortem estimates by morphometric analyses. Data indicate heterogeneous regional distribution of mechanical lung strain, which could influence the differential cellular compensatory response following right and left PNX.

lung resection; compensatory lung growth; high-resolution computed tomography scan; lobar tissue volume; mechanical lung strain; dog

EXPERIMENTAL LUNG RESECTION (pneumonectomy, PNX) mimics the loss of functional lung units in chronic parenchymal disease and is a reproducible model for studying the extent and mechanisms of the adaptive response in the remaining normal lung. After PNX, increased mechanical strain imposed on the remaining lung is a potent stimulus for compensatory tissue responses, leading to lung expansion, recruitment of physiological reserves, and partial to complete normalization of gas-exchange capacity (6, 11, 23). Initiation of compensatory lung growth in adult dogs depends on exceeding a threshold of mechanical strain, as occurs after resection of ~58% of total lung mass by right PNX but not after ~42% resection by left PNX (7, 8); minimization of lung strain blunts compensatory lung expansion as well as cellular and physiological responses (12, 13, 27). At postmortem, we routinely observed uneven shape changes among the lobes that remain after PNX. We theorized that regional distribution of post-PNX mechanical strain is heterogeneous, depending on the amount and location of lung tissue removed and on the relative rigidity and asymmetry of mediastinal structures, such as heart, major vessels, and ligaments, that could restrict the direction and extent of regional expansion. Heterogeneous strain distribution could, in turn, influence regional compensatory cellular growth (19, 30). To assess the in vivo heterogeneity of regional lung volume after PNX, we performed high-resolution computed tomography (CT) scans at a constant transpulmonary pressure in adult foxhounds that had undergone either left or right PNX and reconstructed each remaining lobe to examine anatomic patterns of lobar expansion. We compared air and tissue volumes of each remaining lobe with that in the corresponding lobe of Sham control animals to determine the in vivo distribution of air and tissue among lobes. In addition, some of the animals had received retinoic acid (RA) after PNX as part of a separate study, and we were able to examine the effect of RA treatment on regional distribution of lung volume.

MATERIALS AND METHODS

Experimental groups. The Institutional Animal Care and Use Committee at the University of Texas Southwestern Medical Center approved all procedures. Male adult foxhounds (~1 yr old) underwent either right PNX (~58% resection, $n = 12$) or left PNX (~42% resection, $n = 11$) under general anesthesia by previously described procedures (23). Of the animals undergoing right PNX, three received *all-trans*-retinoic acid (RA; Sigma, St. Louis, MO) beginning 1 day after surgery (2 mg/kg po, 4 days/wk over 4 mo) and three received placebo (oil diluent only) by the same regimen as part of a separate study (4, 28). CT scan was performed during the fourth postoperative month. Details of drug administration and its physiological as well as morphological effects have been described elsewhere (4, 28). Six additional animals underwent right PNX but received no drug treatment and were scanned ~1 yr after surgery. Of the animals undergoing left PNX, five received RA and six received placebo by the same regimen described above; CT scan was performed during the fourth postoperative month. Separate adult control animals underwent thoracotomy without PNX (Sham group, $n = 7$), received no drug treatment, and were scanned ~10 mo after surgery.

CT scan. We conducted the spiral CT scan using a GE high-speed CTI scanner at 3 × 3-mm collimation. Animals were fasted overnight, sedated with acepromazine (0.15 mg/kg sc) and atropine (0.023 ml/kg sc), and anesthetized with propofol (4–8 mg/kg iv for induction followed by 0.4 $mg \cdot kg^{-1} \cdot min^{-1}$ infusion). Animals were intubated with a cuffed endotracheal tube, placed in the supine position on the

Address for reprint requests and other correspondence: C. C. W. Hsia, Pulmonary and Critical Care Medicine, Univ. of Texas Southwestern Medical Center, 5323 Harry Hines Blvd., Dallas, TX 75390-9034.

 8750-7587/04 $5.00 Copyright © 2004 the American Physiological Society

Downloaded from http://jap.physiology.org/ by 10.220.33.1 on September 22, 2017

CT table, and mechanically ventilated (model 607, Harvard Apparatus, Millis, MA) at a tidal volume of 15 ml/kg and a respiratory rate sufficient to eliminate spontaneous breathing effort. Airway pressure was monitored. A scout image was obtained first to ensure the field of scan included the entire lung from the lung apex to the costophrenic angle. Before each imaging sequence, the lungs were hyperinflated with three tidal breaths; this was followed by passive expiration to functional residual capacity. The endotracheal tube was then connected to a calibrated syringe set to deliver a volume of air that had been previously determined in each animal to inflate the lungs to a transpulmonary pressure of 20 cmH_2O. In each animal, the static transpulmonary pressure-lung volume relationship was determined in duplicate under anesthesia on at least one (but sometimes multiple) occasion before CT scan. On each occasion, we measured the change in transpulmonary pressure with a given volume inflation delivered from end expiration by a calibrated syringe; absolute lung volumes were also measured from the dilution of either helium or methane with a rebreathing technique (4, 9). After the lung was inflated with this predetermined volume, the breath was held for ~30 s while CT images were obtained; afterward, the animal was switched back to the respirator. Images were reconstructed at consecutive 1-mm intervals resulting in ~300 images per animal.

Analysis of CT images. We analyzed images using Object-Image version 1.6.2 (public domain software). We used density thresholding to outline the area occupied by the lung on each image; this excluded conducting blood vessels larger than 1–2 mm in diameter. The trachea and next three generations of large conducting airways were excluded manually by marking them with the background color in each CT image in which they appeared. Lung volume in each image is equal to the product of its area and thickness (1 mm); total lung volume was calculated from the sum of the volume of all images. The CT densities (in Houndsfeld units) of tracheal air and of skeletal muscle were measured as estimates of air and tissue density, respectively, and used to partition the total lung volume into air and tissue volumes, since the average CT density of the lung is directly proportional to the ratio of tissue and air. Lobar fissures were identified by following serial images; we used these fissures and customized image analysis algorithms developed by us to partition the lobes of each lung. Figure 1 illustrates the demarcation of the fissure separating two adjacent lobes. Lobar tissue and air volumes were calculated as below:

$$\text{Lobar tissue volume} = \frac{\text{lobar density} - \text{air density}}{\text{muscle density} - \text{air density}} \times \text{lobar volume} \quad (1)$$

$$\text{Lobar air volume} = \text{total volume} - \text{tissue volume} \quad (2)$$

Estimates of tissue volume by CT scan included the volume of alveolar septa as well as extraseptal airways and blood vessels <1–2 mm in diameter (i.e., resolution limit of the CT image).

Statistical analysis. Measurements were normalized by body weight and expressed as means ± SE. Volumes of each lobe were expressed as a fraction of the total volume of each lung. In addition, measurements from PNX animals were expressed as a fraction of the corresponding lobar values in Sham controls. We performed comparisons between groups by one-way ANOVA and Fisher's multiple comparisons test (StatView version 5.0; SAS Institute, Cary, NC). A P value of <0.05 was considered significant.

RESULTS

Lobar geometry after right or left PNX. Figure 2 illustrates representative images of the thorax after right and left PNX compared with Sham controls, showing mediastinal shift and enlargement of the remaining lung. Figure 3 illustrates the three-dimensional reconstruction of each lobe in different anatomic views. The normal dog has three lobes in the left lung [upper (cranial), middle, and lower (caudal)] and four lobes in the right lung [upper (cranial), middle, lower (caudal), and cardiac]. After right PNX, the left upper and middle lobes expanded across the midline anterior to the heart, whereas the left lower lobe expanded across the midline posterior to the heart. After left PNX, the remaining right upper and cardiac lobes expanded above and below the heart, respectively, whereas the remaining right middle and lower lobes showed relatively little expansion.

Lobar volumes after right PNX. Table 1 shows partition of air and tissue volumes among different lobes in the normal left lung (Sham) and in the remaining left lung of animals following right PNX. Animals receiving RA showed slightly lower lobar air and tissue volumes compared with placebo or untreated groups; differences did not reach statistical significance except for tissue volume in the left upper lobe, which was 12.5% lower ($P < 0.05$ vs. placebo). For subsequent lobar comparison with Sham animals (Fig. 4), data from RA- and placebo-treated groups were pooled. Volumes of the left upper, middle, and lower lobes comprised 27, 18, and 55% of the total volume of the left lung, respectively; these relative volumes were unchanged after right PNX (29, 22, and 49%, respectively; $P > 0.05$ vs. Sham). After right PNX, lobar volumes of the left lung expressed as a ratio relative to corresponding values from Sham animals were 2.2-fold (upper lobe), 2.6-fold

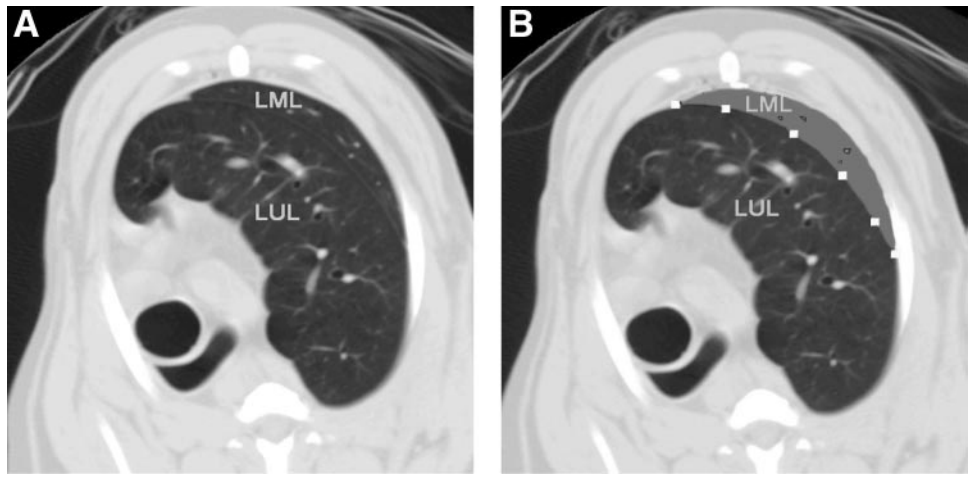


Fig. 1. Computed tomography (CT) image from a dog after right pneumonectomy (PNX) (*A*) showing identification of the minor fissure between left upper (LUL) and middle (LML) lobes by cubic spline (*B*; indicated by □) and separation of the areas occupied by LML from that of LUL.

Downloaded from http://jap.physiology.org/ by 10.220.33.1 on September 22, 2017

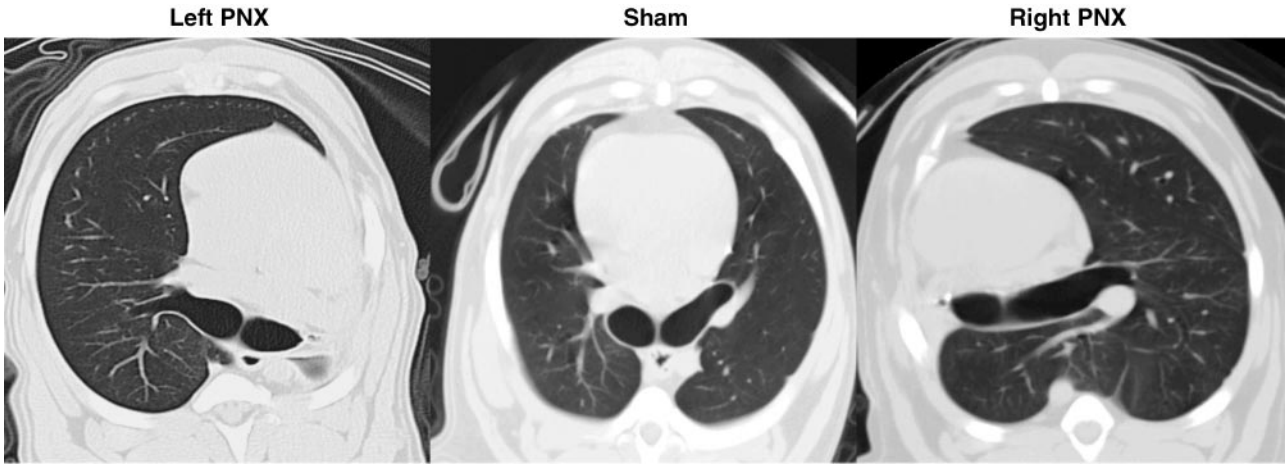


Fig. 2. Representative CT images at the level of the carina showing mediastinal shift and enlargement of the remaining lung after left PNX (*left*) or right PNX (*right*) compared with Sham controls (*middle*).

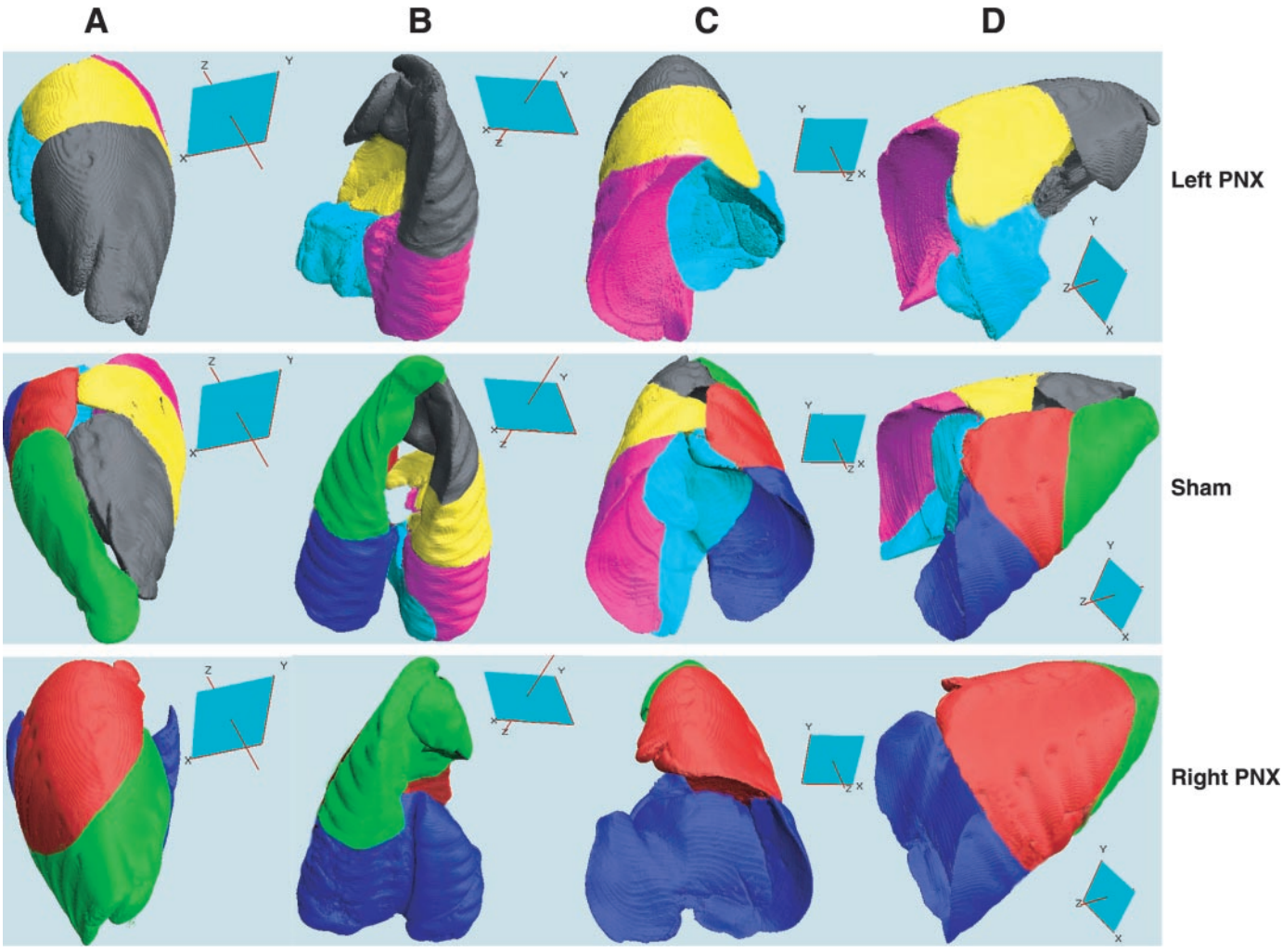


Fig. 3. Three-dimensional reconstruction of both lungs in Sham animals, the right lung in animals after left PNX, and the left lung in animals after right PNX, shown in 4 views oriented by their coordinate axes. *A*: anterior view. *B*: posterior view. *C*: caudal view. *D*: anterior-oblique view. Green: LUL or cranial lobe. Red: LML. Blue: left lower or caudal lobe (LLL). Gray: right upper or cranial lobe (RUL). Yellow: right middle lobe (RML). Magenta: right lower or caudal lobe (RLL). Aqua: right cardiac lobe (RCL).

Downloaded from http://jap.physiology.org/ by 10.220.33.1 on September 22, 2017

Table 1. *Lobar volumes in the normal left lung and after right PNX*

	Sham	Right PNX	Right PNX
Drug treatment	None	Placebo or none	Retinoic acid
n	7	9	3
Body wt, kg	25.2±0.7	27.4±0.9*	25.2±0.7[a]
		Tissue volume, ml/kg	
Left upper lobe	1.0±0.1†‡	2.4±0.1*†‡	2.1±0.2*†‡[a]
Left middle lobe	0.6±0.1‡§	1.6±0.2*‡§	1.7±0.1*‡§
Left lower lobe	2.3±0.1†§	4.5±0.2*†§	4.3±0.3*†§
Total left lung	3.9±0.3	8.5±0.5*	8.1±0.6*
		Air volume, ml/kg	
Left upper lobe	9.9±0.7†‡	23.0±0.9*†‡	19.3±1.9*‡
Left middle lobe	6.5±0.4‡§	17.3±1.9*‡§	16.1±1.0*‡
Left lower lobe	19.4±1.2†§	36.3±1.8*†§	33.9±1.0*†§
Total left lung	35.8±2.3	76.6±3.7*	69.3±3.9*
		Tissue volume/total volume	
Left upper lobe	0.088±0.004‡	0.095±0.006	0.097±0.002‡
Left middle lobe	0.082±0.004‡	0.087±0.006‡	0.096±0.001‡
Left lower lobe	0.105±0.003†§	0.113±0.008†	0.114±0.008†§
Total left lung	0.096±0.003	0.101±0.007	0.105±0.005

Values are means ± SE; n = no. of animals. PNX, pneumonectomy. *$P < 0.05$ vs. sham group; †$P < 0.05$ vs. left middle lobe; ‡$P < 0.05$ vs. left lower lobe; §$P < 0.05$ vs. left upper lobe; [a]$P < 0.05$ vs. placebo (all by ANOVA).

(middle lobe), and 1.9-fold (lower lobe); volume increase was significantly greater for the middle lobe compared with the lower lobe ($P < 0.05$). Lobar air and tissue volumes showed similar patterns of change as total lobar volume (Fig. 4).

Volume density of lung tissue (ratio of tissue volume to total volume) estimated by CT scan was significantly (19–29%) higher in the left lower lobe than in the upper or middle lobes in all groups (Table 1). There was no significant difference in tissue volume density between PNX and Sham groups or between RA- and placebo-treated groups.

Lobar volumes after left PNX. Table 2 shows partition of air and tissue volumes among different lobes in the normal right lung (Sham group) and in the remaining right lung of animals after left PNX. Animals receiving RA after left PNX showed slightly lower lobar air and tissue volumes compared with placebo or untreated groups, but differences did not reach statistical significance. Therefore, data from RA- and placebo-treated groups were pooled for subsequent comparison with Sham animals (Fig. 5). In Sham animals, volume of the right upper, middle, lower, and cardiac lobes comprised 20, 25, 40, and 15% of the total volume of the right lung, respectively; corresponding values were not significantly different after left PNX (29, 15, 35, and 20%, respectively; $P > 0.05$ left PNX vs. Sham group). After left PNX, lobar air and tissue volumes of the right lung expressed as a ratio relative to corresponding Sham values (Fig. 5) were 2.2 (upper lobe), 0.9 (middle lobe), 1.3 (lower lobe), and 2.1 (cardiac lobe); volume increased significantly in the upper and cardiac lobes ($P < 0.05$) but not in the middle or lower lobes.

In all groups, volume density of tissue estimated by CT scan was significantly (14–29%) higher in the right lower and cardiac lobes than in the right upper or middle lobes (Table 2). In Sham animals, tissue volume densities in corresponding lobes of the right and left lung are similar (Tables 1 and 2). However, tissue volume densities were systematically lower in animals after left PNX than in corresponding lobes of Sham animals, reaching statistical significance for the right middle, lower, and cardiac lobes (~15–25% lower) but not for right upper lobe (~10–12% lower). There was no significant difference in tissue volume density between RA- and placebo-treated groups after left PNX.

Changes in overall lung volumes. In Sham animals, average tissue and air volumes of the right lung constituted 57% of the total respective volume of both lungs. After right PNX, average air and tissue volumes of the remaining left lung increased proportionally (108 and 115%, respectively, above Sham left lung); thus the overall volume density of tissue remained unchanged (Table 1). After left PNX, the average air volume of the remaining right lung was 54% higher than in the right lung of Sham animals, and tissue volume was only 21% higher; therefore, the overall volume density of tissue was significantly (18%) lower (Table 2).

DISCUSSION

Summary of findings. Divergent patterns of regional lung expansion were observed in adult dogs in response to different forms of lung resection. After right PNX, mediastinal shift is prominent and all remaining lobes expanded significantly (1.9- to 2.6-fold of that in corresponding Sham lobes), with the

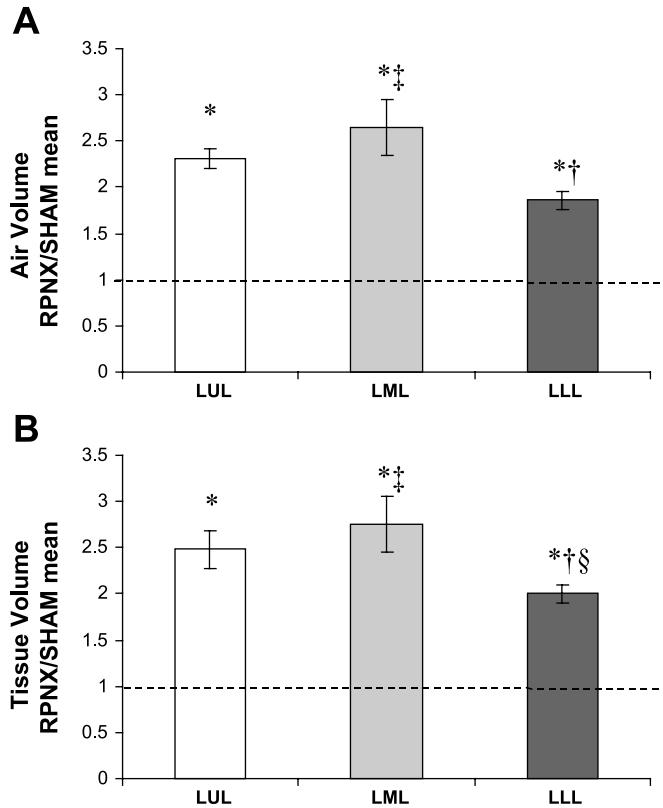


Fig. 4. Relative change in lobar air volume (*A*) and tissue volume (*B*) in the remaining left lung following right PNX (RPNX, $n = 12$) expressed as a fraction of the mean value in corresponding lobes of Sham animals ($n = 7$). Values are means ± SE. *$P < 0.05$ vs. 1.0 (dashed line; corresponding lobe in Sham controls). §$P < 0.05$ vs. LUL. †$P < 0.05$ vs. LML. ‡$P < 0.05$ vs. LLL by ANOVA. All remaining lobes expanded significantly but not uniformly after right PNX.

Downloaded from http://jap.physiology.org/ by 10.220.33.1 on September 22, 2017

Table 2. *Lobar volumes in the normal right lung and after left PNX*

Group	Sham	Left PNX	Left PNX
Drug treatment	None	Placebo	Retinoic acid
n	7	5	6
Body wt, kg	25.2±0.6	25.4±0.9	25.8±0.8
	Tissue volume, ml/kg		
Right upper lobe	0.9±0.1‡	1.8±0.1*†‡	1.6±0.1*†‡
Right middle lobe	1.2±0.2‡ψ	0.9±0.1‡§ψ	0.8±0.1‡§ψ
Right lower lobe	2.3±0.1†§ψ	2.5±0.1†§ψ	2.4±0.2†§ψ
Right cardiac lobe	0.8±0.1†‡	1.4±0.1*†‡	1.4±0.1*†‡
Total right lung	5.2±0.5	6.6±0.4*	6.2±0.5*
	Air volume, ml/kg		
Right upper lobe	10.2±1.5‡	23.2±1.0*†‡ψ	21.4±0.9*†‡ψ
Right middle lobe	12.5±1.5‡ψ	12.8±1.6‡§	11.5±0.7‡§ψ
Right lower lobe	19.9±1.4†§ψ	27.8±0.4†§ψ	26.3±0.9†§ψ
Right cardiac lobe	7.2±0.5†‡	16.0±1.1*‡§	15.4±1.1*†‡§
Total right lung	49.8±4.9	79.8±4.1*	74.6±3.6*
	Tissue volume/total volume		
Right upper lobe	0.080±0.003‡ψ	0.072±0.003‡ψ	0.070±0.005
Right middle lobe	0.087±0.004‡ψ	0.067±0.002*‡ψ	0.065±0.005*‡ψ
Right lower lobe	0.103±0.003†§	0.083±0.002*†§	0.082±0.005*†
Right cardiac lobe	0.099±0.002†§	0.083±0.003*†§	0.084±0.006*†
Total right lung	0.094±0.002	0.077±0.002*	0.076±0.005*

Values are means ± SE; *n* = no. of animals. **P* < 0.05 vs. Sham group; †*P* < 0.05 vs. right middle lobe; ‡*P* < 0.05 vs. right lower lobe; §*P* < 0.05 vs. right upper lobe; ψ*P* < 0.05 vs. right cardiac lobe (all by ANOVA). There were no significant differences between retinoic acid and placebo groups.

greatest expansion occurring in the left upper and middle lobes. In contrast, after left PNX, the remaining right upper and cardiac lobes enlarged approximately twofold across the midline above and below the heart to reconstitute a compliant cardiac fossa, whereas the remaining right middle and lower lobes did not expand significantly. These anatomic changes reflect nonuniform in vivo distribution of intrathoracic mechanical strain after PNX. Lobar expansion is greater in magnitude and uniformity after right PNX than after left PNX, related to differential anatomic restrictions imposed by the asymmetry and relative rigidity of the heart, mediastinal great vessels, and cardiophrenic ligaments.

Density gradients were analyzed to quantify regional volume density of tissue. After right PNX, lobar tissue volume increased in proportion to air volume; hence, volume density of tissue was unchanged, consistent with morphometric evidence of compensatory growth of acinar tissue (8). After left PNX, lobar tissue volume either did not increase or the increase lagged behind that in air volume, consistent with previous morphometric reports showing a lack of compensatory growth of alveolar tissue (7, 13). Administration of RA after PNX had little effect on CT-derived lobar air and tissue volumes or their regional distributions.

Comparison with literature and technical considerations. Density gradients from thoracic CT scan have been utilized to partition changes of lung air and tissue volumes (2) in the assessment of emphysema (3), idiopathic pulmonary fibrosis (1, 5), growth of pulmonary nodules (26), and acute respiratory distress syndrome (16–18, 21). Changes in volume distribution between upper and lower lobes have been reported in patients with acute lung injury (17). However, few studies have utilized this method for assessing regional lung growth in vivo. We previously utilized CT scan to assess regional lung volume in foxhounds that had undergone right PNX as puppies and subsequently been raised to adulthood (24). Results show that the post-PNX volume increase in the remaining lung is greater in the midthoracic region than in the caudal region near the costophrenic angle, a finding consistent with the present data. We had also utilized CT scan to study the effects of preventing post-PNX lateral lung expansion in adult dogs by using space-occupying inflated silicone prosthesis to replace the resected lung (27). In the presence of an inflated prosthesis, post-PNX volume expansion is preferentially blunted in the midlung region compared with animals with a deflated prosthesis. Our previous CT studies were done with an older generation scanner at a lower resolution and without volumetric imaging and hence could not reliably resolve lobar fissures; this technical limitation has been overcome with spiral CT scan. In these animals, we did not obtain CT scan before surgery. In subsequent cohorts (Sham and after right PNX), we found no difference in lobar distribution of air or tissue volume when CT scan was performed at 4 or 10 mo after surgery (unpublished observations).

Although spiral CT scan does not eliminate cardiogenic motion artifacts (20), such artifacts occur in all animals and do

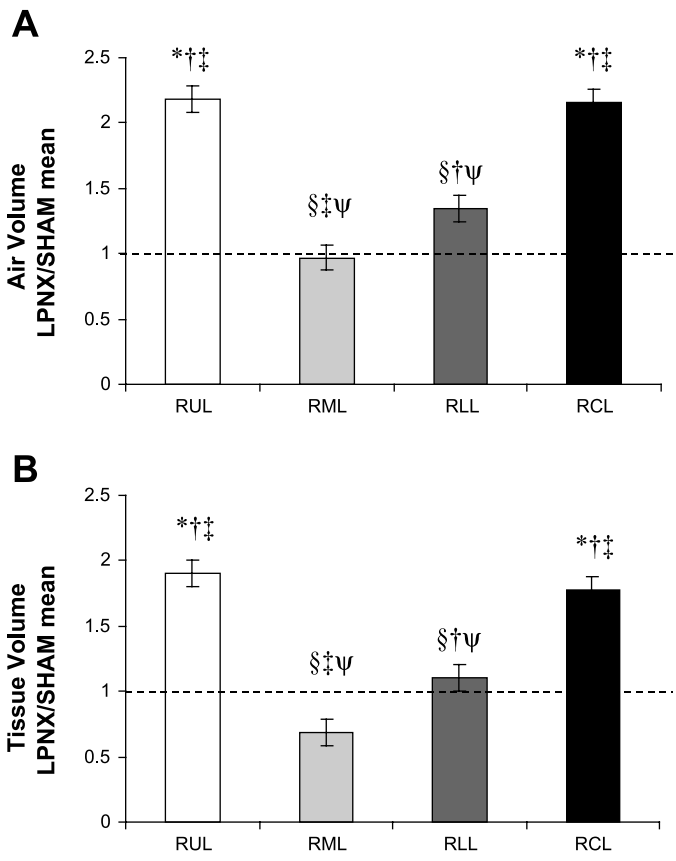


Fig. 5. Relative change in lobar air volume (*A*) and tissue volume (*B*) in the remaining right lung after left PNX (LPNX, *n* = 11) expressed as a fraction of the mean value in corresponding lobes of Sham animals (*n* = 7). Values are means ± SE. **P* < 0.05 vs. 1.0 (dashed line, corresponding lobe in Sham controls). §*P* < 0.05 vs. right upper lobe (RUL). †*P* < 0.05 vs. RML. ‡*P* < 0.05 vs. RLL. ψ*P* < 0.05 vs. right cardiac lobe (RCL) by ANOVA. Volume of RUL and RCL doubled after LPNX, whereas that of RML and RLL did not expand significantly.

Downloaded from http://jap.physiology.org/ by 10.220.33.1 on September 22, 2017

not alter systematic comparisons among groups. In vivo lung volume obtained by CT scan is systematically larger than that measured postmortem after tracheal instillation of fixatives at 25 cmH_2O of hydrostatic pressure (4, 28). The difference between air-filled and liquid-filled lungs can be at least partly attributed to differences in thoracic compliance at the time of lung inflation and variable loss of pressure with time as well as residual elastic recoil and septal refolding in the fixed lung (29). Because CT-derived tissue volume includes not just alveolar septa but also small blood vessels and airway tissue up to ~1–2 mm in diameter, i.e., the resolution limit of the scan, CT-derived tissue volume is systematically higher than alveolar septal volume (tissue + capillary blood) measured by morphometric methods in postmortem fixed lungs. Nonetheless, there are strong correlations between these two independent estimations of total air and tissue volumes in 21 of the animals in which measurements by both methods are available (Fig. 6). These correlations lend support to the use of CT scan to track parenchyma growth in vivo.

Regional post-PNX compensatory response. Sekhon and Thurlbeck (22) found in growing rats after left PNX that volume expansion was greatest in the postcaval (cardiac) lobe followed by the middle lobe of the remaining right lung. In post-PNX dogs, we routinely observed at postmortem irregular shape changes in the remaining lung, particularly in the upper and cardiac lobes after left PNX and in the upper and lower lobes after right PNX. These lobes show odd-looking projections of tissue that herniate across the apical midline (upper lobe) or wrap around the caudal esophagus (lower or cardiac lobe), where the lack of rigid ligaments allow lung expansion in response to chronic mechanical stress. In our previous morphometric analysis, we did not separately analyze each lobe. We routinely fixed the lung by tracheal instillation of fixatives at a constant hydrostatic pressure (7, 8). Each lung was then divided into upper and lower strata while the airway pressure was maintained. The upper stratum consisted of the upper and middle lobes. The lower stratum consisted of either the lower lobe alone (left lung) or lower and cardiac lobes (right lung). This division was employed because the upper and middle lobes are often incompletely separated; forced separation causes loss of airway pressure and hence variability in lung volume measurement by the saline immersion method (25). Using this sampling method, we reported that, in adult dogs after left PNX, volume of septal tissue measured by morphometry was not different from that in the same lung of normal animals and average volume density of alveolar septum per unit lung volume was significantly reduced (~0.12 in normal dogs and ~0.09 after left PNX) (7). Because blood volume in the remaining lung increases post-PNX and CT-derived tissue volume includes volume of blood in small vessels, the 27% higher absolute tissue volume in the remaining lung after left PNX is not surprising; however, average volume density of tissue remains 18% lower than that in normal animals (~0.094 in Sham dogs and ~0.077 after left PNX) (Table 2), consistent with morphometric results. Post-PNX reduction in tissue volume density was greater in the middle and lower lobes (~20–25%) than in the upper and cardiac lobes (~10–15%) (Fig. 4). Because the upper and lower stratum each contained one lobe that expanded significantly and one that did not, grouping two lobes into one stratum may obscure interlobar differences in structural adap-

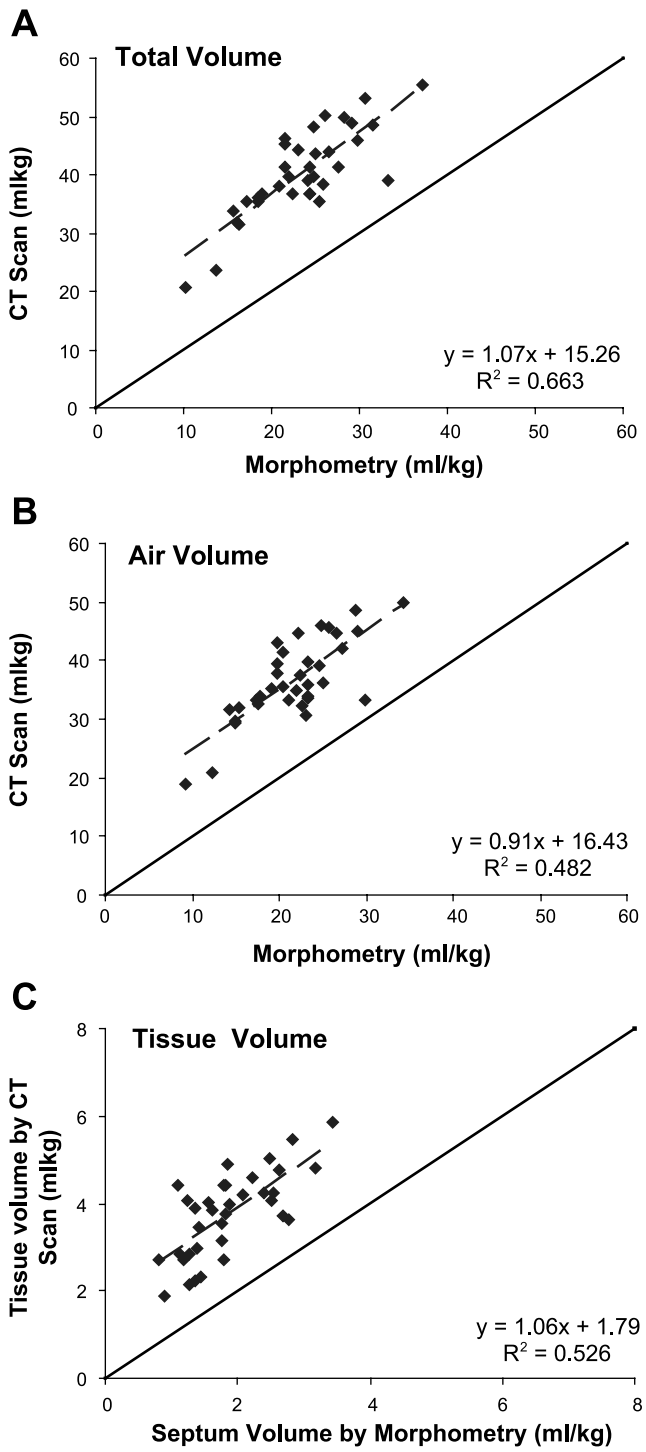


Fig. 6. Correlation of lung volumes measured in vivo by CT scan at 20 cmH_2O transpulmonary pressure and at postmortem by morphometry after tracheal instillation of fixatives at 25 cmH_2O airway pressure in 21 animals in which both measurements are available. Fixed lungs were sectioned serially, and the total volume and alveolar septal volumes were estimated by point counting; differences between these two volumes were taken as air volume. Each data point represents volume of either a lobe ($n = 6$) or a stratum ($n = 15$): upper stratum includes upper and middle lobes; lower stratum includes the left lower lobe alone or the right lower and cardiac lobes. *A*: total volume. *B*: air volume. *C*: tissue volume (by CT scan) and volume of alveolar septum (by morphometry). Solid line, identity. Dashed line, regression through data range.

Downloaded from http://jap.physiology.org/ by 10.220.33.1 on September 22, 2017

tation even though no overall compensatory alveolar growth was evident by either CT scan or morphometry. We now use a modified postmortem sampling method to measure volume of each lobe separately by point counting (29).

In adult dogs after right PNX, the remaining lobes expanded more uniformly and to a greater extent than after left PNX; hence, grouping left upper and middle lobes into the upper stratum would not bias morphometric analysis. The more vigorous lobar expansion after right PNX is associated with proportional increases in alveolar septal cell volumes in the remaining lobes, such that volume density of alveolar septa per unit lung volume remained unchanged (average 0.11–0.12), leading to a 61% increase in lung diffusing capacity estimated by both morphometric as well as physiological methods (8, 10). In parallel with these prior findings, CT-derived tissue volume density after right PNX is also not different from that in Sham controls (average ~0.10) (Table 1). The pattern of volume expansion to structural growth after different types of lung resection suggests that compensatory tissue response is influenced not only by the magnitude of regional mechanical strain but also by its distribution.

Effect of RA. Exogenous RA has been reported to enhance postnatal alveolar septation (14) and minimize alveolar loss in emphysematous rats (15). In adult dogs treated with RA after right PNX, lung volumes measured at a given airway pressure antemortem or postmortem were not significantly altered compared with matched placebo controls (4, 28), in parallel with CT-derived estimates. RA treatment after right PNX selectively enhances the compensatory increase in alveolar capillary and endothelial cell volumes, with a ~26% higher volume of alveolar septa and 37% increase in volume density of the septum compared with placebo controls (28); these moderate alveolar structural changes are not reflected in CT-derived tissue volume, again likely due to inclusion of small conducting structures in the latter measurement. After left PNX, neither CT analysis nor morphometry shows any effect of RA treatment on the compensatory response. RA treatment did not alter the lobar volume distribution after left or right PNX.

In conclusion, we report distinct patterns of lobar expansion after left and right PNX, which reflect nonuniform regional distribution of mechanical lung strain stemming from constraints imposed by rigid mediastinal structures such as the heart, great vessels, and ligaments. The increase in mechanical lung strain is greater in magnitude and more uniformly distributed after right than after left PNX. Heterogeneity in regional strain distribution may influence local histological response and compensatory alveolar growth after lung resection. Direct verification of regional pressures would require implantation of multiple pleural and/or parenchymal markers that have not yet been done. CT-derived estimates of air and tissue volumes correlate with estimates obtained postmortem in the same lungs fixed by tracheal instillation, supporting the utility of CT scan in following parenchyma growth in vivo. However, spiral CT scan cannot reliably resolve fine structural perturbations at the alveolar level.

ACKNOWLEDGMENTS

We thank Daryn Clyburn for assistance with animal care; Derek Lowe, Melanie Bishop, and Cynthia Proper for technical assistance with CT scan; Dr. Roderick McColl for assistance with data transfer; and the Department of Radiology and the staff of Aston Ambulatory Care Center for making the facilities available.

GRANTS

This study was supported by National Heart, Lung, and Blood Institute Grants R01 HL-40070, HL-54060, HL-45716, and HL-62873.

REFERENCES

1. **Coxson HO, Hogg JC, Mayo JR, Behzad H, Whittall KP, Schwartz DA, Hartley PG, Galvin JR, Wilson JS, and Hunninghake GW.** Quantification of idiopathic pulmonary fibrosis using computed tomography and histology. *Am J Respir Crit Care Med* 155: 1649–1656, 1997.
2. **Coxson HO, Mayo JR, Behzad H, Moore BJ, Verburgt LM, Staples CA, Pare PD, and Hogg JC.** Measurement of lung expansion with computed tomography and comparison with quantitative histology. *J Appl Physiol* 79: 1525–1530, 1995.
3. **Coxson HO, Rogers RM, Whittall KP, D'Yachkova Y, Pare PD, Sciurba FC, and Hogg JC.** A quantification of the lung surface area in emphysema using computed tomography. *Am J Respir Crit Care Med* 159: 851–856, 1999.
4. **Dane DM, Yan X, Tamhane RM, Johnson RL Jr, Estrera AS, Hogg DC, Hogg RT, and Hsia CCW.** Retinoic acid-induced alveolar cellular growth does not improve function after right pneumonectomy. *J Appl Physiol* 96: 1090–1096, 2004.
5. **Hartley PG, Galvin JR, Hunninghake GW, Merchant JA, Yagla SJ, Speakman SB, and Schwartz DA.** High-resolution CT-derived measures of lung density are valid indexes of interstitial lung disease. *J Appl Physiol* 76: 271–277, 1994.
6. **Hsia CCW, Carlin JI, Ramanathan M, Cassidy SS, and Johnson RL Jr.** Estimation of diffusion limitation after pneumonectomy from carbon monoxide diffusing capacity. *Respir Physiol* 83: 11–21, 1991.
7. **Hsia CCW, Fryder-Doffey F, Stalder-Navarro V, Johnson RL Jr, and Weibel ER.** Structural changes underlying compensatory increase of diffusing capacity after left pneumonectomy in adult dogs. *J Clin Invest* 92: 758–764, 1993. [Corrigenda. *J Clin Invest* 93: 1994, p. 913.]
8. **Hsia CCW, Herazo LF, Fryder-Doffey F, and Weibel ER.** Compensatory lung growth occurs in adult dogs after right pneumonectomy. *J Clin Invest* 94: 405–412, 1994.
9. **Hsia CCW, Herazo LF, Ramanathan M, Claassen H, Fryder-Doffey F, Hoppeler H, and Johnson RL Jr.** Cardiopulmonary adaptations to pneumonectomy in dogs. III. Ventilatory power requirements and muscle structure. *J Appl Physiol* 76: 2191–2198, 1994.
10. **Hsia CCW, Herazo LF, Ramanathan M, and Johnson RL Jr.** Cardiopulmonary adaptations to pneumonectomy in dogs. IV. Membrane diffusing capacity and capillary blood volume. *J Appl Physiol* 77: 998–1005, 1994.
11. **Hsia CCW, Herazo LF, Ramanathan M, Johnson RL Jr, and Wagner PD.** Cardiopulmonary adaptations to pneumonectomy in dogs. II. Ventilation-perfusion relationships and microvascular recruitment. *J Appl Physiol* 74: 1299–1309, 1993.
12. **Hsia CCW, Johnson RL Jr, Wu EY, Estrera AS, Wagner H, and Wagner PD.** Reducing lung strain after pneumonectomy impairs diffusing capacity but not ventilation-perfusion matching. *J Appl Physiol* 95: 1370–1378, 2003.
13. **Hsia CCW, Wu EY, Wagner E, and Weibel ER.** Preventing mediastinal shift after pneumonectomy impairs regenerative alveolar tissue growth. *Am J Physiol Lung Cell Mol Physiol* 281: L1279–L1287, 2001.
14. **Massaro GD and Massaro D.** Postnatal treatment with retinoic acid increases the number of pulmonary alveoli in rats. *Am J Physiol Lung Cell Mol Physiol* 270: L305–L310, 1996.
15. **Massaro GD and Massaro D.** Retinoic acid treatment abrogates elastase-induced pulmonary emphysema in rats. *Nat Med* 3: 675–677, 1997. [Corrigenda. *Nat Med* 3: July 1997, p. 805]
16. **Puybasset L, Cluzel P, Chao N, Slutsky AS, Coriat P, and Rouby JJ.** A computed tomography scan assessment of regional lung volume in acute lung injury. The CT Scan ARDS Study Group. *Am J Respir Crit Care Med* 158: 1644–1655, 1998.
17. **Puybasset L, Cluzel P, Gusman P, Grenier P, Preteux F, and Rouby JJ.** Regional distribution of gas and tissue in acute respiratory distress syndrome. I. Consequences for lung morphology. The CT Scan ARDS Study Group. *Intensive Care Med* 26: 857–869, 2000.
18. **Puybasset L, Gusman P, Muller JC, Cluzel P, Coriat P, and Rouby JJ.** Regional distribution of gas and tissue in acute respiratory distress syndrome. III. Consequences for the effects of positive end-expiratory pressure. The CT Scan ARDS Study Group Adult Respiratory Distress Syndrome. *Intensive Care Med* 26: 1215–1227, 2000.

Downloaded from http://jap.physiology.org/ by 10.220.33.1 on September 22, 2017

19. **Rannels DE.** Role of physical forces in compensatory growth of the lung. *Am J Physiol Lung Cell Mol Physiol* 257: L179–L189, 1989.
20. **Reinhardt JM and Hoffman EA.** Quantitative pulmonary imaging: spatial and temporal considerations in high-resolution CT. *Acad Radiol* 5: 539–546, 1998.
21. **Rouby JJ, Puybasset L, Cluzel P, Richecoeur J, Lu Q, and Grenier P.** Regional distribution of gas and tissue in acute respiratory distress syndrome. II. Physiological correlations and definition of an ARDS Severity Score. CT Scan ARDS Study Group. *Intensive Care Med* 26: 1046–1056, 2000.
22. **Sekhon HS and Thurlbeck WM.** A comparative study of postpneumonectomy compensatory lung response in growing male and female rats. *J Appl Physiol* 73: 446–451, 1992.
23. **Takeda S, Hsia CCW, Wagner E, Ramanathan M, Estrera AS, and Weibel ER.** Compensatory alveolar growth normalizes gas exchange function in immature dogs after pneumonectomy. *J Appl Physiol* 86: 1301–1310, 1999.
24. **Takeda S, Wu EY, Epstein RH, Estrera AS, and Hsia CCW.** In vivo assessment of changes in air and tissue volumes after pneumonectomy. *J Appl Physiol* 82: 1340–1348, 1997.
25. **Weibel ER, Kistler GS, and Scherle WF.** Practical stereological methods for morphometric cytology. *J Cell Biol* 30: 23–38, 1966.
26. **Wormanns D, Kohl G, Klotz E, Marheine A, Beyer F, Heindel W, and Diederich S.** Volumetric measurements of pulmonary nodules at multi-row detector CT: in vivo reproducibility. *Eur Radiol* 14: 86–92, 2004.
27. **Wu EY, Hsia CC, Estrera AS, Epstein RH, Ramanathan M, and Johnson RL Jr.** Preventing mediastinal shift after pneumonectomy does not abolish physiological compensation. *J Appl Physiol* 89: 182–191, 2000.
28. **Yan X, Bellotto DJ, Foster DJ, Johnson RL Jr, Hagler HH, Estrera AS and Hsia CC.** Retinoic acid induces nonuniform alveolar septal growth after right pneumonectomy. *J Appl Physiol* 96: 1080–1089, 2004.
29. **Yan X, Polo Carbayo JJ, Weibel ER, and Hsia CC.** Variation of lung volume after fixation when measured by immersion or Cavalieri method. *Am J Physiol Lung Cell Mol Physiol* 284: L242–L245, 2003.
30. **Zhang S, Garbutt V, and McBride JT.** Strain-induced growth of the immature lung. *J Appl Physiol* 81: 1471–1476, 1996.



Downloaded from http://jap.physiology.org/ by 10.220.33.1 on September 22, 2017